Available online at www.sciencedirect.com
ScienceDirect
International Journal of Heat and Mass Transfer 50 (2007) 2170–2181
International Journal of HEAT and MASS TRANSFER
www.elsevier.com/locate/ijhmt

Solution of a stationary inverse heat conduction problem by means of Trefftz non-continuous method

Michał J. Ciałkowski [a], Andrzej Frąckowiak [a], Krzysztof Grysa [b,*]

[a] The Poznań University of Technology, 5 Maria Skłodowska-Curie Sq., 60-965 Poznań, Poland
[b] The Kielce University of Technology, Al. 1000-lecia Panstwa Polskiego 7, 25-314 Kielce, Poland

Received 13 April 2006; received in revised form 1 November 2006
Available online 22 January 2007

Abstract

In the paper, the non-continuous FEM with Trefftz base functions (FEMT) applied to direct and inverse problem of heat conduction equation has been presented. For the finite number of base functions in each finite element the temperature field becomes non-continuous on the border between elements. This non-continuity has been decreased with the penalty function added to optimised functional. The numerical entropy distribution and energy dissipation function have been analysed on the common boundaries of elements. Increasing the number of base functions in the finite element substantially decreases the inaccuracies of direct and inverse problem solution.

Keywords: Inverse problem; Non-continuous solution

1. Introduction

The classic finite element method (FEM) ensures continuity of an approximate solution on the neighbouring elements when applied to solving a partial differential equation. Giving the continuity postulate up leads to non-continuous Galerkin method [4,5]. A non-continuous solution between elements can be also obtained from a new definition of functional leading to the FEM. Namely, the functional can be completed with terms directly referring to discontinuity of the solution between elements. Such approach will be presented in the paper.

In FEM the base functions in general do not satisfy the given differential equation. However, in particular cases for some linear equation one can introduce the base functions (called Trefftz functions) that fulfill the given differential equation identically. Then, functional leading to the FEMT (finite element method with Trefftz functions) may have other interpretation than usually accepted one. For heat conduction equation the functional is interpreted as mean-square sum of defects in heat flux flowing from element to element [2], with condition of continuity of temperature in the common nodes of elements. Full continuity between elements is not ensured because of finite number of base functions in each element. However, even the condition of temperature continuity in nodes may be weakened. We can assume no temperature continuity at any point between elements. Instead, we can minimize defect of energy dissipation between elements or numerical entropy production [1,3], because discontinuity of heat flux between elements implies discontinuity of energy dissipation and entropy production. Minimizing these three discontinuities may lay down new criteria for finding an approximate solution of heat conduction equation. In the paper, numerical defects of dissipation function as well as numerical defects of entropy production intensity will be presented and discussed for solutions obtained when minimizing the heat flux discontinuity between finite elements.

2. Problem formulation

The main advantage of Trefftz functions is that they satisfy differential equation identically. Applying the FEMT

* Corresponding author. Tel.: +48 605063336; fax: +48 413424536.
E-mail address: grysa@poczta.onet.pl (K. Grysa).

0017-9310/$ - see front matter © 2006 Elsevier Ltd. All rights reserved.
doi:10.1016/j.ijheatmasstransfer.2006.11.030

Nomenclature

a_i, b_i	coefficients
α, α_{ij}	penalty coefficients, $\alpha > 0$
δ	distance from the x-axis to line of nodes (Fig. 4)
$\delta T_i = T_+ - T_-$	temperature jump in the node x_i or at the border Γ_{ij}
$\delta q_i = \dot{q}_+ - \dot{q}_-$	heat flux jump in the node x_i
δH^1	norm of the approximate solution
δq_n	norm of the numerical heat flux defect
$\delta \Psi_c$	norm of the numerical energy dissipation defect
$\delta \sigma_c$	norm of the numerical entropy production defect
Γ_w	a sum of all boundaries between the neighbouring elements
$I(T)$	classical functional (formula (3))
λ	heat conductivity coefficient
$\dot{q}$	heat flux
$\dot{q}_{n+} - \dot{q}_{n-}$	heat flux jump at the border Γ_{ij}
$Q(T)$	functional including Trefftz functions (formula (4))
σ	functional of entropy production
T	temperature
$\widetilde{T}$	approximate solution
Θ_0, Θ_1	boundary values of temperature
ψ	energy dissipation functional
x	spatial variable
x_i	nodes

one ought to choose a proper functional. Minimizing the functional leads to the best solution.

Consider the problem of looking for a proper functional for the following one-dimensional problem:

$$\frac{\mathrm{d}^2 u}{\mathrm{d}x^2} = g(x), \quad x \in (0,1), \quad u(0) = u_0, \quad u(1) = u_1 \tag{1}$$

We can write the problem by means of homogeneous equation

$$\frac{\mathrm{d}^2 T}{\mathrm{d}x^2} = 0, \quad T = u - \left(\frac{\mathrm{d}^2}{\mathrm{d}x^2}\right)^{-1} g, \quad T(0) = \Theta_0, \quad T(1) = \Theta_1 \tag{1a}$$

Dividing the interval $\langle 0;1\rangle$ into subintervals we can find a general solution of the problem in each subinterval in the form

$$T_i = a_i x + b_i, \quad x_i < x < x_{i+1}, \quad i = 1,2,\ldots,N,$$
$$x_1 = 0, \quad x_{N+1} = 1 \tag{2}$$

In general case, the function T does not have to be continuous in the nodes x_i. In order to find the coefficients a_i, b_i we can construct two functionals that take into consideration discontinuity of temperature between elements:

– the classic one:

$$I(T) = \int_0^1 \left(\frac{\mathrm{d}T}{\mathrm{d}x}\right)^2 \mathrm{d}x + \alpha \sum_i (T_+ - T_-)_i^2 = \sum_i \int_{x_i}^{x_{i+1}} \left(\frac{\mathrm{d}T}{\mathrm{d}x}\right)^2 \mathrm{d}x + \alpha \sum_i (T_+ - T_-)_i^2, \quad \alpha > 0 \tag{3}$$

– a functional including the Trefftz functions properties and energy conservation between elements:

$$Q(T) = \sum_i \left[(\dot{q}_+ - \dot{q}_-)_i^2 + \alpha (T_+ - T_-)_i^2\right], \quad \alpha > 0, \qquad \dot{q} = -\lambda \frac{\mathrm{d}T}{\mathrm{d}x} \tag{4}$$

The term $\alpha(T_+ - T_-)^2$ has a character of a penalty function and vanishes for continuous solution. In further considerations we will show that to obtain exact (continuous) solution for 1D case it is enough to assume $\alpha > 0$.

Consider minimizing the functionals (3) and (4) with respect to the coefficients a_i, b_i with the boundary conditions taken into account and the interval $\langle 0,1\rangle$ divided into three parts as shown in Fig. 1.

Minimizing the functional (3) with respect to the coefficients a_1, a_2, a_3 and b_2 leads to the system of three algebraic equations with the following solution:

$$a_1 = a_2 = a_3 = \frac{\alpha}{1+\alpha} \cdot (\Theta_1 - \Theta_2),$$
$$b_2 = \frac{1}{2}\Theta_0\left(1 - \frac{\alpha}{1+\alpha}\right) + \frac{1}{2}\Theta_1\left(1 - \frac{\alpha}{1+\alpha}\right) \tag{5}$$

Consider two particular cases:

(a) $\alpha \to 0$ (Fig. 2a); then

$$a_1 = a_2 = a_3 = 0, \quad b_2 = \frac{\Theta_0 + \Theta_1}{2},$$
$$\delta_1 T = \delta_2 T = \frac{1}{2}(\Theta_0 - \Theta_1) \tag{6}$$

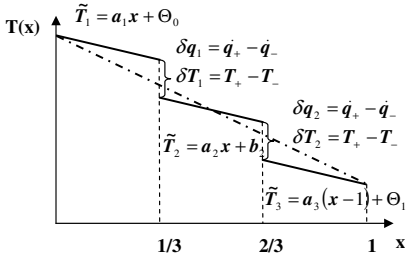

Fig. 1. Analytical solution (dashed line) and discontinuous solution (piecewise continuous line).

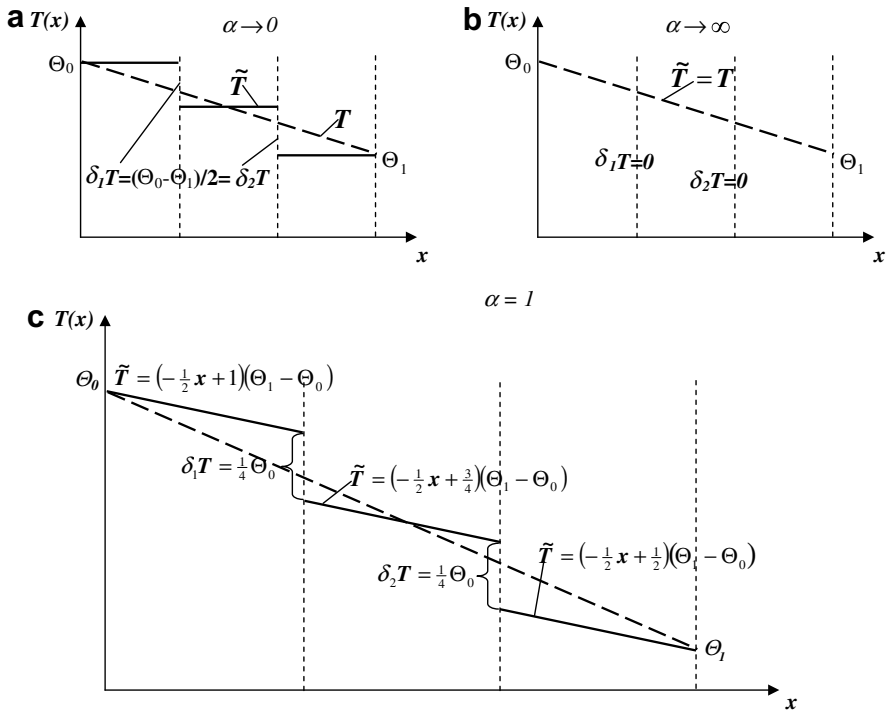

Fig. 2. Solutions obtained when minimizing the functional (3).

(b) $\alpha \to \infty$ (Fig. 2b); then

$$a_1 = a_2 = a_3 = \Theta_1 - \Theta_0, \quad b_2 = \Theta_0, \quad \delta_1 T = \delta_2 T = 0 \tag{7}$$

Hence, for the case (a) we obtain the discontinuous solution (Fig. 2a) and for the case (b) continuous solution (Fig. 2b).

For finite values of $\alpha > 0$ we arrive at a discontinuous solution. Diagram of the solution for $\alpha = 1$ is shown in Fig. 2c.

Minimizing the functional $Q(T)$ (see formula (4)) with respect to coefficients a_1, a_2, a_3 and b_2 leads to a system of three algebraic equations with the following solution:

$$a_1 = a_2 = a_3 = \Theta_1 - \Theta_0, \quad b_2 = \Theta_0 \qquad \text{for } \alpha > 0 \tag{8}$$

The same solution was obtained above for classic functional (3) but for infinite value of α. It is an important advantage of the functional (4) when compared to functional (3).

If $\alpha > 0$ then solution of the system (8) is a continuous function which is plotted as a dashed line (analytical solution) in Fig. 1.

For $\alpha = 0$ we obtain $a_1 = a_2 = a_3$ and b_2 indetermined (an indeterminate solution).

Now we modify the functional (4) introducing numerical defect of entropy production or of energy dissipation instead of numerical defect of heat flux, $\dot{q}_+ - \dot{q}_-$. We can define the following functionals:

– functional of entropy production with discontinuous heat flux [3]

$$\sigma = \sum_i \left[\int_{\Gamma_i} \left(\underbrace{\frac{\dot{q}_+}{T_+} - \frac{\dot{q}_-}{T_-}}_{\substack{\text{entropy} \\ \text{discontinuity}}} \right)^2 \mathrm{d}\Gamma + \alpha \int_{\Gamma_i} \left(\underbrace{\dot{q}_+ - \dot{q}_-}_{\substack{\text{heat flux} \\ \text{discontinuity}}} \right)^2 \mathrm{d}\Gamma \right] = \min, \quad \dot{q} \equiv \dot{q}_n = -\lambda \frac{\partial T}{\partial n} \tag{9}$$

– functional of entropy production with discontinuous temperature [3]

$$\sigma = \sum_i \left[\int_{\Gamma_i} \left(\underbrace{\frac{\dot{q}_+}{T_+} - \frac{\dot{q}_-}{T_-}}_{\substack{\text{entropy} \\ \text{discontinuity}}} \right)^2 \mathrm{d}\Gamma + \alpha \int_{\Gamma_i} \left(\underbrace{T_+ - T_-}_{\substack{\text{temperature} \\ \text{discontinuity}}} \right)^2 \mathrm{d}\Gamma \right] = \min, \quad \alpha > 0 \tag{10}$$

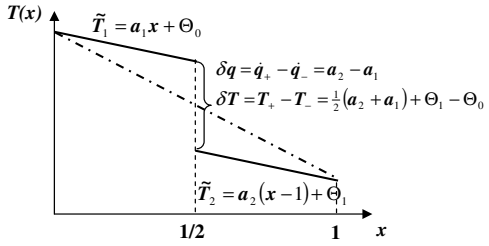

Fig. 3. Analytical solution (dashed line) and discontinuous solution (piecewise continuous line).

– energy dissipation functional with discontinuous temperature

$$\psi = \sum_i \left[\int_{\Gamma_i} (\ln T_+ \dot{q}_+ - \ln T_- \dot{q}_-)^2 \, d\Gamma + \alpha \int_{\Gamma_i} (T_+ - T_-)^2 \, d\Gamma \right] = \min, \quad \alpha > 0 \tag{11}$$

As an example let us consider temperature distribution in the interval $\langle 0, 1 \rangle$ divided into two subintervals (Fig. 3) The heat flux/temperature discontinuity on the border between elements may be minimized by using the entropy production intensity functional (formulas (9) and (10), respectively).

Introducing temperature distribution in the intervals $\langle 0, 0.5 \rangle$ and $\langle 0.5, 1 \rangle$ into the functionals (9) and (10) we arrive at the following form of the entropy production intensity functional:

– in the case of formula (9)

$$\sigma = \left(\frac{a_1}{\frac{a_1}{2} + \Theta_0} - \frac{a_2}{\frac{-a_2}{2} + \Theta_1} \right)^2 + \alpha (a_1 - a_2)^2 \tag{12}$$

– in the case of formula (10)

$$\sigma = \left(\frac{a_1}{\frac{a_1}{2} + \Theta_0} - \frac{a_2}{\frac{-a_2}{2} + \Theta_1} \right)^2 + \alpha [\Theta_1 - \Theta_0 - (a_1 + a_2)/2]^2 \tag{13}$$

Minimizing the functional (12) with respect to the coefficients a_1 and a_2 and neglecting trivial solutions leads to the following solution for $\alpha > 0$:

$$a_1 = a_2 = \Theta_1 - \Theta_0 \tag{14}$$

Then $\delta T = 0$ and $\sigma = 0$, i.e. we obtain as a solution continuous function describing temperature with no discontinuity on the border between elements.

For $\alpha = 0$ (i.e. for the functional without penalty function) we arrive to an equation with infinite number of solutions

$$a_1 a_2 = a_1 \Theta_1 - a_2 \Theta_2$$

Minimizing the functional (13) with respect to the coefficients a_1 and a_2 and neglecting trivial solutions lead for $\alpha > 0$ to the solution (14), too.

Thus, it is clear from the two examples that minimizing the entropy production intensity functional with term describing temperature/heat flux discontinuity $(\alpha(T_+ - T_-)^2$ or $\alpha(\dot{q}_+ - \dot{q}_-)^2$, respectively) leads to unique solution.

Presented functionals (formulas (4), (9) and (10)) can be easily formulated for 2D and 3D problems. Then the coefficient $\alpha > 0$ depends on the border between elements and is to be calculated. In this case the procedure of minimizing the functional leads to non-linear problem. The functionals (4), (9) and (10) can be then written down in the same form, namely:

$$\varphi = \sum_i \left[\int_{\Gamma_i} (F_+ - F_-)^2 \, d\Gamma + \alpha_i \int_{\Gamma_i} (T_+ - T_-)^2 \, d\Gamma \right], \quad \alpha_i > 0 \tag{15}$$

Here, for $\alpha_i > 0$

$$\varphi = \begin{cases} Q & \text{if } F = \dot{q}_n = -\lambda \frac{\partial}{\partial n} T \\ \sigma & \text{if } F = \frac{\dot{q}_n}{T} = -\lambda \frac{\partial}{\partial n} \ln T \\ \psi & \text{if } F = \dot{q} \ln T = -\lambda \frac{\partial}{\partial n} T (\ln T - 1) \end{cases} \tag{16}$$

The functional (19) includes discontinuity

- of the function describing temperature or heat flux if $F = \dot{q}_n$;
- of the entropy production if $F = \dot{q}_n / T$;
- of the dissipation function if $F = \dot{q}_n \ln T$.

3. Analysis of 2D problem solution

Let us consider an inverse problem for stationary 2D heat conduction problem. It will be solved by using the Trefftz function (in this case – harmonic functions). The Trefftz functions satisfy the governing differential equation and therefore it is convenient to use them as base functions in FEM. Because of finite number of the base functions in each element we can require continuity of temperature in the nodal points only. Between the nodes the temperature is not continuous.

Instead of this requirement we can minimize a functional (similar to that one for 1D case – comp. formula (4)) of a form [3]:

$$I(T) = \sum_{ij} \left[\int_{\Gamma_{ij}} (\dot{q}_{n+} - \dot{q}_{n-})^2 \, d\Gamma_{ij} + \alpha_{ij} \int_{\Gamma_{ij}} (T_+ - T_-)^2 \, d\Gamma_{ij} \right], \quad \alpha_{ij} > 0 \tag{17}$$

The procedure of finding the inverse problem solution consists in reconstructing an unknown boundary condition when measured values of temperature along a line inside the body (continuous problem) or at chosen points of the line (discrete problem) are known. In Fig. 4 the points are chosen on a line parallel to $0x$ axis (distant for δ from

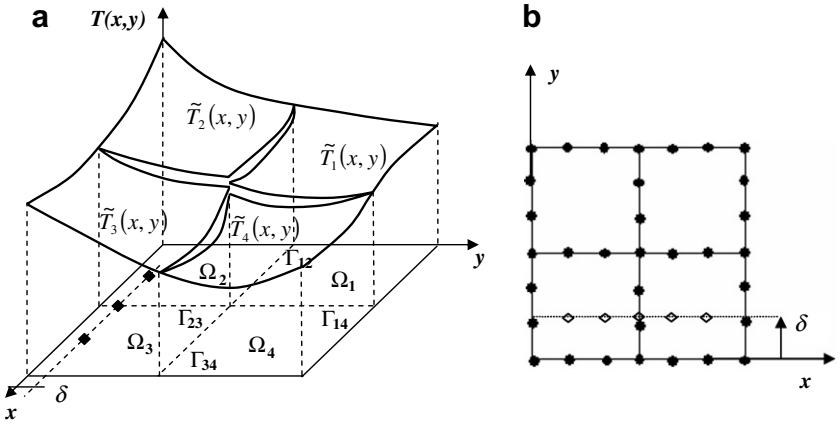

Fig. 4. (a) Temperature distribution approximated with non-continuous elements. (b) Nodes (black dots) and points with given values of temperature (white dots).

the axis). In a particular case for $\delta = 0$ an inverse problem becomes a direct one. For numerical calculation the considered domain (a square, see Fig. 4) is divided into four finite elements. In each element 12 Trefftz functions are taken as base functions.

Visualization of non-continuous solution of a 2D problem is presented in Fig. 4a. The points with given values of temperature are shown in Fig. 4b.

To solve an inverse problem (as well as a direct one) two functionals can be used:

– for a problem with pointwise continuous temperature between elements [2]:

$$I(T) = \sum_{ij} \int_{\Gamma_{ij}} (\dot{q}_{n+} - \dot{q}_{n-})^2 \, \mathrm{d}\Gamma_{ij} \tag{18}$$

– for a problem with non-continuous temperature between elements ($\alpha_{ij} = \alpha = \text{const.}$, generalized functional (4))

$$Q(T) = \sum_{ij} \left[\int_{\Gamma_{ij}} (\dot{q}_{n+} - \dot{q}_{n-})^2 \mathrm{d}\Gamma_{ij} + \alpha \int_{\Gamma_{ij}} (T_+ - T_-)^2 \mathrm{d}\Gamma_{ij} \right], \quad \alpha > 0 \tag{19}$$

Approximate solution fully satisfies boundary conditions at nodal points.

In order to test the method the analytical solution is adopted in the following form:

$$T_e(x,y) = \frac{\cos\left(\frac{\pi}{2}x\right)\sinh\left(\frac{\pi}{2}(1-y)\right)}{\sinh\left(\frac{\pi}{2}\right)} \tag{20}$$

Accuracy of the approximate solution (let us denote it as $\widetilde{T}$) is estimated in the norm δH^1 (see formula (21)). Also the accuracy of the heat flux δq_n (see (22)) entropy production $\delta\sigma_c$ (see (23)) and energy dissipation $\delta\Psi_c$ (see (24)) is investigated. Signs plus and minus denote sides of the border between two elements.

The formulas read:

– norm of the approximate solution:

$$\delta H^1 = \left(\frac{\int_\Omega \left[(\widetilde{T} - T_e)^2 + \left(\frac{\partial \widetilde{T}}{\partial x} - \frac{\partial T_e}{\partial x} \right)^2 + \left(\frac{\partial \widetilde{T}}{\partial y} - \frac{\partial T_e}{\partial y} \right)^2 \right] \mathrm{d}\Omega}{\int_\Omega \left[T_e^2 + \left(\frac{\partial T_e}{\partial x} \right)^2 + \left(\frac{\partial T_e}{\partial y} \right)^2 \right] \mathrm{d}\Omega} \right)^{1/2} \cdot 100\ [\%] \tag{21}$$

– norm of the numerical heat flux defect:

$$\delta q_n = \left(\frac{\int_{\Gamma_w} \left[\left(\frac{\partial \widetilde{T}}{\partial n} \right)_+ - \left(\frac{\partial \widetilde{T}}{\partial n} \right)_- \right]^2 \mathrm{d}\Gamma}{\int_{\Gamma_w} \left[\frac{1}{2} \left(\left(\frac{\partial \widetilde{T}}{\partial n} \right)_+ + \left(\frac{\partial \widetilde{T}}{\partial n} \right)_- \right) \right]^2 \mathrm{d}\Gamma} \right)^{1/2} \cdot 100\ [\%] \tag{22}$$

– norm of the numerical entropy production defect:

$$\delta\sigma_c = \left(\frac{\int_{\Gamma_w} \left[\left(\frac{1}{\widetilde{T}} \cdot \frac{\partial \widetilde{T}}{\partial n} \right)_+ - \left(\frac{1}{\widetilde{T}} \cdot \frac{\partial \widetilde{T}}{\partial n} \right)_- \right]^2 \mathrm{d}\Gamma}{\int_{\Gamma_w} \left[\frac{1}{2} \left(\left(\frac{1}{\widetilde{T}} \cdot \frac{\partial \widetilde{T}}{\partial n} \right)_+ + \left(\frac{1}{\widetilde{T}} \cdot \frac{\partial \widetilde{T}}{\partial n} \right)_- \right) \right]^2 \mathrm{d}\Gamma} \right)^{1/2} \cdot 100\ [\%] \tag{23}$$

– norm of the numerical energy dissipation defect:

$$\delta\Psi_c = \left(\frac{\int_{\Gamma_w} \left[\left(\ln\left(\widetilde{T}\right) \frac{\partial \widetilde{T}}{\partial n} \right)_+ - \left(\ln\left(\widetilde{T}\right) \frac{\partial \widetilde{T}}{\partial n} \right)_- \right]^2 \mathrm{d}\Gamma}{\int_{\Gamma_w} \left[\frac{1}{2} \left(\left(\ln\left(\widetilde{T}\right) \frac{\partial \widetilde{T}}{\partial n} \right)_+ + \left(\ln\left(\widetilde{T}\right) \frac{\partial \widetilde{T}}{\partial n} \right)_- \right) \right]^2 \mathrm{d}\Gamma} \right)^{1/2} \cdot 100\ [\%] \tag{24}$$

The boundary Γ_w is a sum of all boundaries between the neighbouring elements.

In the numerical example the functional (19) is used. In the case of pointwise continuous temperature on Γ_w the procedure of minimizing the functional (19) diminishes discontinuities of temperature between nodes. The applied method of penalty function with the parameter $\alpha > 0$ has an effect on decreasing discontinuities of temperature, heat flux, numerical entropy production and energy dissipation on Γ_w. Values of the norm δH^1 in the considered square as a function of parameter α and distance δ of thermoelements from the $0x$ axis ($\delta = 0$ denotes a direct problem) are presented in Table 1 for pointwise continuous problem as well as for the non-continuous one. Data from Table 1 are presented in graphical form in Fig. 5 for pointwise continuous problem and in Fig. 6 for the non-continuous one.

Notice, that for the pointwise continuous temperature α practically does not effect the solution for $\delta < 0.5$ (points with given temperature values are in the first layer of elements). For non-continuous FEMT small parameter α generally increases temperature inaccuracies while big α decreases them. High values of the norm δH^1 for $\alpha = 0.001$ and $\delta = 0.20$ as well as for $\alpha = 1000$ and $\delta = 0.60$ result from temperature discontinuity for $x = 0.5$ and too small number of base functions.

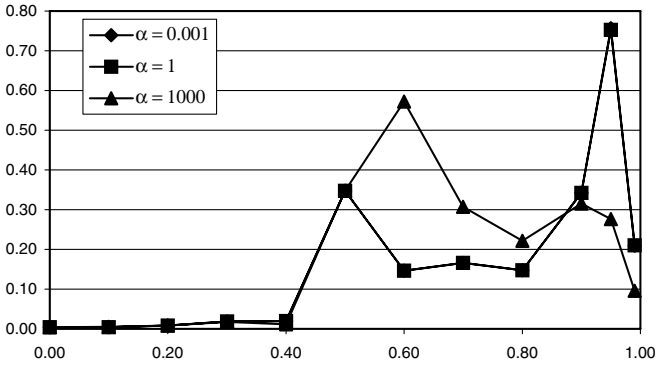

Fig. 5. Norm δH^1 for different values of α (FEMT pointwise continuous, 12 base functions).

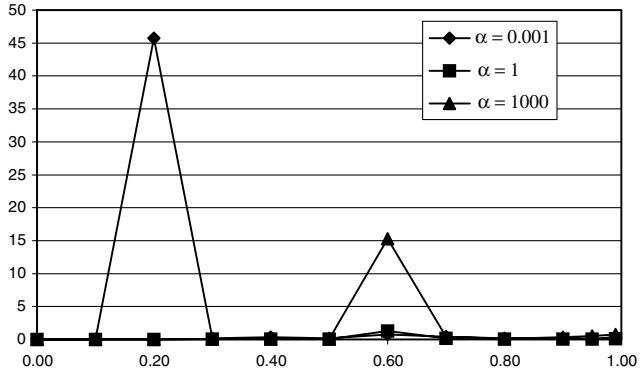

Fig. 6. Norm δH^1 for different values of α (FEMT non-continuous, 12 base functions).

3.1. Pointwise continuous problem

Errors of the heat flux, entropy production and energy dissipation on the border between elements for the intersection $x = 0.5$ as functions of parameter α and distance δ are presented in Table 2. The results analogous to those from Table 2 but for the intersection $y = 0.5$ are presented in Table 3. In Fig. 7 the results presented in Table 2 are shown in graphic form for $\alpha = 1$. Graphic form of the results from Table 3 looks likewise.

Again we see that small parameter α generally increases heat flux, entropy production and energy dissipation defects; big α decreases them. Only for $\delta = 0.5$ the norms are relatively high; it is a result of taking data from the border between elements and insufficient number of base functions.

3.2. Non-continuous problem

Errors of the heat flux, entropy production and energy dissipation on the border between elements for the intersection $x = 0.5$ as functions of parameter α and distance δ are

Table 1
Norm δH^1 as a function of the distance δ from the boundary $y = 0$ (12 base functions in an element)

δ	FEMT pointwise continuous			FEMT non-continuous		
	$\alpha = 0.001$	$\alpha = 1$	$\alpha = 1000$	$\alpha = 0.001$	$\alpha = 1$	$\alpha = 1000$
0.00	0.0042	0.0042	0.0042	0.0207	0.0141	0.0161
0.10	0.0046	0.0046	0.0047	0.0852	0.0153	0.0168
0.20	0.0081	0.0081	0.0081	45.7378	0.0208	0.0204
0.30	0.0184	0.0184	0.0178	0.1805	0.0376	0.0333
0.40	0.0199	0.0199	0.0115	0.3494	0.0603	0.0749
0.50	0.3471	0.3471	0.3471	0.1856	0.0383	0.0523
0.60	0.1459	0.1460	0.5723	0.7475	1.2637	15.2711
0.70	0.1655	0.1656	0.3076	0.3954	0.1711	0.3990
0.80	0.1479	0.1479	0.2220	0.1931	0.0786	0.1323
0.90	0.3426	0.3425	0.3153	0.2029	0.0753	0.3492
0.95	0.7568	0.7527	0.2762	0.1052	0.0679	0.5004
0.99	0.2097	0.2101	0.0958	0.3669	0.1173	0.7800

Table 2
The norms $\delta q_n, \delta\sigma_c, \delta\Psi_c$ as functions of the distance δ from the boundary $y = 0$ for $\alpha = 0.001$; 1; 1000

δ	Heat flux δq_n (%)			Entropy $\delta\sigma_c$ (%)			Energy dissipation $\delta\Psi_c$ (%)		
	$\alpha = 0.001$	$\alpha = 1$	$\alpha = 1000$	$\alpha = 0.001$	$\alpha = 1$	$\alpha = 1000$	$\alpha = 0.001$	$\alpha = 1$	$\alpha = 1000$
0.00	0.027	0.027	0.027	0.027	0.027	0.028	0.027	0.027	0.027
0.10	0.017	0.017	0.017	0.015	0.015	0.015	0.019	0.019	0.018
0.20	0.027	0.027	0.026	0.030	0.030	0.029	0.026	0.026	0.026
0.30	0.092	0.092	0.088	0.108	0.108	0.104	0.085	0.085	0.081
0.40	0.028	0.028	0.019	0.030	0.030	0.017	0.027	0.027	0.020
0.50	0.196	0.196	0.198	0.230	0.230	0.236	0.182	0.182	0.180
0.60	0.040	0.040	0.260	0.050	0.050	0.318	0.036	0.036	0.234
0.70	0.037	0.038	0.117	0.046	0.046	0.143	0.033	0.034	0.104
0.80	0.343	0.343	0.120	0.397	0.398	0.147	0.319	0.319	0.108
0.90	0.467	0.465	0.042	0.555	0.553	0.034	0.427	0.425	0.045
0.95	1.108	1.098	0.047	1.314	1.303	0.042	1.014	1.006	0.049
0.99	0.032	0.033	0.140	0.038	0.039	0.161	0.030	0.030	0.130

Γ_w is here the intersection $x = 0.5$ (FEMT pointwise continuous, 12 base functions in an element).

Table 3
The norms $\delta q_n, \delta\sigma_c, \delta\Psi_c$ as functions of the distance δ from the boundary $y = 0$ for $\alpha = 0.001$; 1; 1000

δ	Heat flux δq_n (%)			Entropy $\delta\sigma_c$ (%)			Energy dissipation $\delta\Psi_c$ (%)		
	$\alpha = 0.001$	$\alpha = 1$	$\alpha = 1000$	$\alpha = 0.001$	$\alpha = 1$	$\alpha = 1000$	$\alpha = 0.001$	$\alpha = 1$	$\alpha = 1000$
0.00	0.020	0.020	0.002	0.020	0.020	0.002	0.021	0.021	0.002
0.10	0.019	0.019	0.002	0.018	0.018	0.002	0.019	0.019	0.002
0.20	0.015	0.015	0.003	0.016	0.016	0.002	0.015	0.015	0.003
0.30	0.019	0.019	0.003	0.017	0.017	0.003	0.019	0.019	0.003
0.40	0.019	0.019	0.007	0.018	0.018	0.005	0.020	0.020	0.007
0.50	0.119	0.119	0.004	0.097	0.097	0.004	0.132	0.132	0.004
0.60	0.028	0.028	1.700	0.017	0.017	1.307	0.033	0.033	1.845
0.70	0.033	0.033	0.019	0.021	0.021	0.016	0.038	0.039	0.020
0.80	0.088	0.088	0.004	0.074	0.074	0.004	0.093	0.093	0.004
0.90	0.128	0.128	0.016	0.097	0.097	0.010	0.142	0.142	0.018
0.95	0.313	0.310	0.014	0.242	0.240	0.008	0.346	0.343	0.016
0.99	0.044	0.044	0.013	0.027	0.027	0.007	0.052	0.052	0.015

Γ_w is here the intersection $y = 0.5$ (FEMT pointwise continuous, 12 base functions in an element).

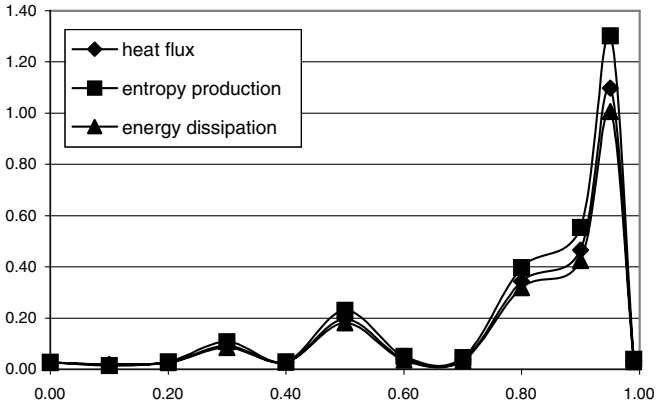

Fig. 7. The norm $\delta q_n, \delta\sigma_c, \delta\Psi_c$ as functions of the distance δ from the boundary $y = 0$ along internal line of intersection $x = 0.5$ for $\alpha = 1$ (FEMT pointwise continuous, 12 base functions in an element).

presented in Table 4. In Table 5 results for $y = 0.5$ are presented. In Fig. 8 the figures from Table 4 for $\alpha = 1$ are shown in graphic form. The graphic form of the results from Table 5 looks likewise.

Again we see that small parameter α generally increases heat flux, entropy production and energy dissipation defects; big α decreases them. Relatively high values of the norms for all α's and $\delta = 0.60$ result from temperature discontinuity on the border between elements and too small number of base functions.

Errors of the entropy production in the intersections $x = 0.5$ and $y = 0.5$ for 24 base functions are presented in Tables 6 and 7.

The numerical results concerning the direct problem show that the differences in norms between solutions obtained with pointwise elements and with non-continuous elements do not exceed 0.01%. Greater differences appear when the inverse problem is being solved. However, it is possible to diminish them essentially by increasing the number of base functions in each element.

The crucial advantage of the non-continuous approach is diminishing inaccuracy of the solution for constant α when enlarging the number of base functions in an element. For $\alpha \in \langle 0.001, 1000\rangle$, 24 base functions and $\delta \in \langle 0, 0.99\rangle$ the relative errors of the entropy production intensity do not exceed 0.029% (comp. Tables 6 and 7).

Table 4
The norms $\delta q_n, \delta\sigma_c, \delta\Psi_c$ as functions of the distance δ from the boundary $y = 0$ for $\alpha = 0.001$; 1; 1000

δ	Heat flux δq_n (%)			Entropy $\delta\sigma_c$ (%)			Energy dissipation $\delta\Psi_c$ (%)		
	$\alpha = 0.001$	$\alpha = 1$	$\alpha = 1000$	$\alpha = 0.001$	$\alpha = 1$	$\alpha = 1000$	$\alpha = 0.001$	$\alpha = 1$	$\alpha = 1000$
0.00	0.006	0.002	0.002	0.011	0.002	0.002	0.006	0.002	0.002
0.10	0.013	0.002	0.002	0.014	0.003	0.002	0.014	0.002	0.002
0.20	10.506	0.002	0.011	10.258	0.003	0.013	11.092	0.002	0.011
0.30	0.032	0.008	0.010	0.051	0.013	0.011	0.041	0.007	0.010
0.40	0.064	0.018	0.041	0.071	0.024	0.045	0.065	0.016	0.039
0.50	0.034	0.003	0.003	0.042	0.007	0.003	0.035	0.003	0.003
0.60	0.113	0.072	11.332	0.115	0.061	12.652	0.118	0.080	10.769
0.70	0.054	0.025	0.099	0.055	0.028	0.111	0.056	0.024	0.094
0.80	0.016	0.003	0.010	0.017	0.006	0.011	0.016	0.002	0.009
0.90	0.031	0.009	0.094	0.033	0.007	0.104	0.032	0.010	0.089
0.95	0.018	0.001	0.073	0.021	0.003	0.081	0.018	0.001	0.070
0.99	0.000	0.003	0.051	0.023	0.005	0.057	0.009	0.003	0.049

Γ_w is here the intersection $x = 0.5$ (FEMT non-continuous, 12 base functions in an element).

Table 5
The norms $\delta q_n, \delta\sigma_c, \delta\Psi_c$ as functions of the distance δ from the boundary $y = 0$ for $\alpha = 0.001$; 1; 1000

δ	Heat flux δq_n (%)			Entropy $\delta\sigma_c$ (%)			Energy dissipation $\delta\Psi_c$ (%)		
	$\alpha = 0.001$	$\alpha = 1$	$\alpha = 1000$	$\alpha = 0.001$	$\alpha = 1$	$\alpha = 1000$	$\alpha = 0.001$	$\alpha = 1$	$\alpha = 1000$
0.00	0.002	0.002	0.002	0.014	0.003	0.002	0.004	0.002	0.002
0.10	0.002	0.002	0.002	0.092	0.003	0.002	0.027	0.002	0.002
0.20	0.738	0.002	0.003	59.461	0.003	0.002	16.102	0.003	0.003
0.30	0.005	0.003	0.003	0.091	0.001	0.003	0.027	0.004	0.003
0.40	0.015	0.004	0.007	0.051	0.003	0.005	0.026	0.006	0.007
0.50	0.008	0.002	0.004	0.021	0.002	0.004	0.013	0.002	0.004
0.60	0.029	0.046	1.700	0.040	0.031	1.307	0.042	0.060	1.845
0.70	0.013	0.005	0.019	0.032	0.007	0.016	0.020	0.008	0.020
0.80	0.003	0.001	0.004	0.020	0.003	0.004	0.008	0.002	0.004
0.90	0.006	0.002	0.016	0.055	0.003	0.010	0.018	0.003	0.018
0.95	0.003	0.001	0.014	0.038	0.002	0.008	0.012	0.001	0.016
0.99	0.001	0.001	0.013	0.020	0.003	0.007	0.006	0.002	0.015

Γ_w is here the intersection $y = 0.5$ (FEMT non-continuous, 12 base functions in an element).

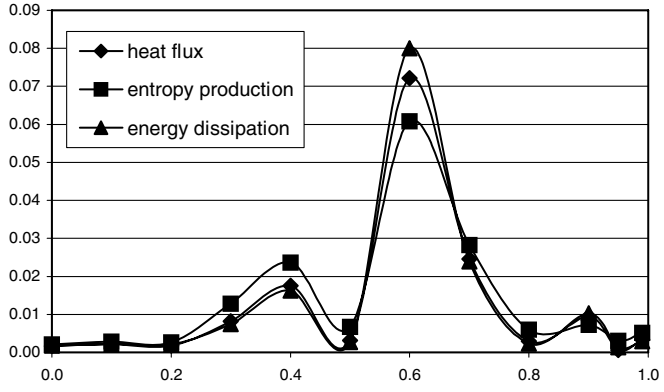

Fig. 8. The norms $\delta q_n, \delta\sigma_c, \delta\Psi_c$ as functions of the distance δ from the boundary $y = 0$ along internal line of intersection $x = 0.5$ for $\alpha = 1$ (FEMT non-continuous, 12 base functions in an element).

4. The FEMT in comparison with the classic FEM

To compare FEM with Trefftz base functions (FEMT) with the classic FEM approach, the FEM solution of the inverse problem for the square considered above is analysed. As a criterion of similarity of the approaches a number of nodes inside or on the boundary of the square is used. For the FEM the elements with four nodes and, consequently, the simplest set of base functions: $\{1, x, y, xy\}$ have been applied.

In the case of FEMT the considered square has been divided into four finite elements with 12 or 24 Trefftz functions as base functions. For 12 Trefftz functions in an element we obtain 33 nodes in the square (24 on the boundary and 9 inside). In the case of 24 of them we have 69 nodes (48 on the boundary and 21 inside).

The variants of number of elements in FEM are presented in Table 8.

Using FEM to solve the inverse problem in the square gives acceptable solution only for the first row of elements. Even for exact values of the given temperature the results are encumbered with relatively high error (comp. Fig. 9).

For the next row of the elements the FEM solution is entirely not acceptable. When the distance δ (comp. Fig. 4) is greater than the size of the element, an instability of the numerical solution appears independently of the number of finite elements. For 16 elements the inaccuracy on the border of the first row of elements is not too high (comp. Fig. 9) but then increases quickly. For 36 and 144

Table 6
The norm of entropy production $\delta\sigma_c$ as functions of the distance δ from the boundary $y = 0$ for $\alpha = 0.001$; 1; 1000

δ	FEMT pointwise continuous			FEMT non-continuous		
	$\alpha = 0.001$	$\alpha = 1$	$\alpha = 1000$	$\alpha = 0.001$	$\alpha = 1$	$\alpha = 1000$
0.00	0.00000	0.00000	0.00000	0.00000	0.00000	0.00000
0.10	0.00000	0.00000	0.00000	0.00038	0.00000	0.00000
0.20	0.00000	0.00000	0.00000	0.00048	0.00004	0.00000
0.30	0.00000	0.00000	0.00000	0.00006	0.00000	0.00000
0.40	0.00000	0.00000	0.00000	0.00040	0.00000	0.00000
0.50	0.00000	0.00000	0.00000	0.00000	0.00000	0.00000
0.60	0.00000	0.00000	0.00000	0.00000	0.00000	0.00000
0.70	0.00000	0.00000	0.00000	0.00030	0.00000	0.00001
0.80	0.00000	0.00000	0.00000	0.00004	0.00000	0.00000
0.90	0.00000	0.00000	0.00000	0.00006	0.00003	0.00000
0.95	0.00000	0.00000	0.00000	0.00428	0.00004	0.00001
0.99	0.00000	0.00000	0.00000	0.00002	0.00001	0.00000

Γ_w is here the intersection $y = 0.5$ (24 base functions in an element).

Table 7
The norm of entropy production $\delta\sigma_c$ as functions of the distance δ from the boundary $y = 0$ for $\alpha = 0.001$; 1; 1000

δ	FEMT pointwise continuous			FEMT non-continuous		
	$\alpha = 0.001$	$\alpha = 1$	$\alpha = 1000$	$\alpha = 0.001$	$\alpha = 1$	$\alpha = 1000$
0.00	0.00000	0.00000	0.00000	0.00000	0.00000	0.00000
0.10	0.00000	0.00000	0.00000	0.00002	0.00000	0.00000
0.20	0.00000	0.00000	0.00000	0.00005	0.00009	0.00000
0.30	0.00000	0.00000	0.00000	0.00002	0.00001	0.00000
0.40	0.00000	0.00000	0.00000	0.00016	0.00000	0.00000
0.50	0.00000	0.00000	0.00000	0.00000	0.00000	0.00000
0.60	0.00000	0.00000	0.00000	0.00000	0.00000	0.00000
0.70	0.00000	0.00000	0.00000	0.00016	0.00000	0.00004
0.80	0.00000	0.00000	0.00000	0.00001	0.00001	0.00000
0.90	0.00000	0.00000	0.00000	0.00001	0.00020	0.00006
0.95	0.00000	0.00000	0.00000	0.00265	0.00029	0.00028
0.99	0.00000	0.00000	0.00000	0.00001	0.00004	0.00002

Γ_w is here the intersection $x = 0.5$ (24 base functions in an element).

Table 8
Number of elements in the FEM and FEMT for comparing the results of calculation for the inverse problem in a square

Total number of elements		Number of the boundary nodes		Number of the internal nodes		Criterion of similarity
FEMT 12 Trefftz functions	FEM	FEMT 12 Trefftz functions	FEM	FEMT 12 Trefftz functions	FEM	
4	16	24	16	9	9	Internal nodes number
4	36	24	24	9	25	Boundary nodes number
FEMT 24 Trefftz functions	FEM	FEMT 24 Trefftz functions	FEM	FEMT 24 Trefftz functions	FEM	
4	144	48	48	21	121	Boundary nodes number

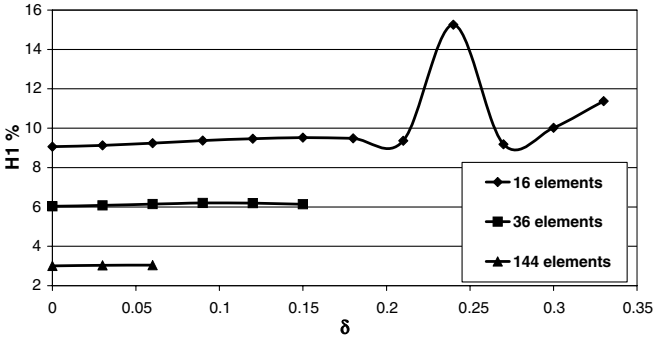

Fig. 9. Norm δH^1 for the FEM solution for different values of δ.

elements one observes violent loss of stability; the calculation error becomes greater than 300%. Paradoxically, the greater number of elements the quicker the instability appears even though the accuracy of solution in the first row of elements becomes better (comp. also Figs. 10–12).

Errors of the heat flux, entropy production and energy dissipation on the border between elements for the intersection $x = 0.5$ as functions of parameter α and distance δ are presented in Figs. 10–12 for the FEM solution for 16, 36 and 144 elements, respectively. The results are similar to those presented in Fig. 9.

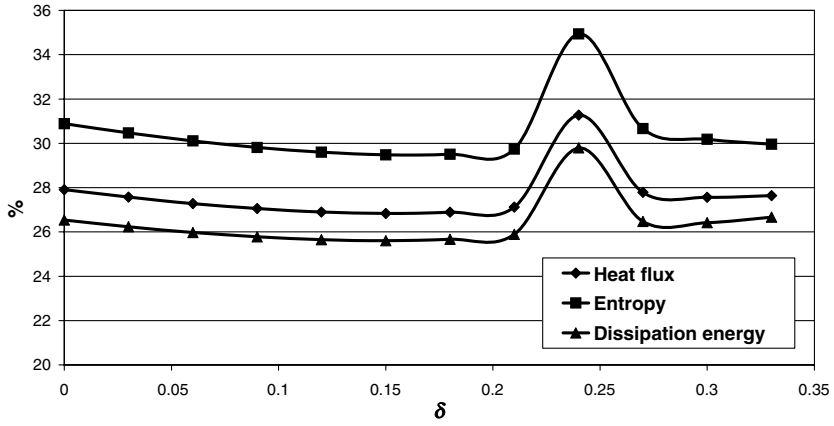

Fig. 10. The norm $\delta q_n, \delta\sigma_c, \delta\Psi_c$ as functions of the distance δ from the boundary $y = 0$ along internal line of intersection $x = 0.5$ for FEM with 16 elements.

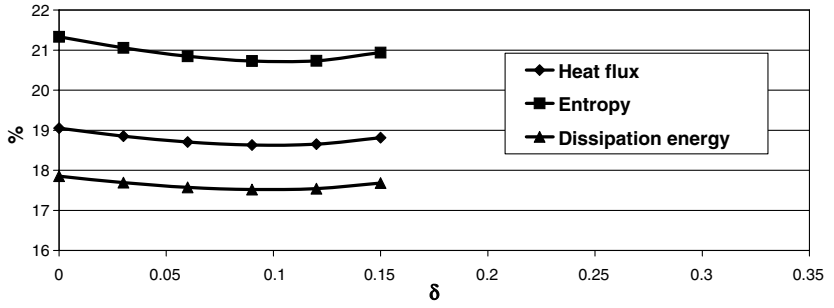

Fig. 11. The norm $\delta q_n, \delta\sigma_c, \delta\Psi_c$ as functions of the distance δ from the boundary $y = 0$ along internal line of intersection $x = 0.5$ for FEM with 36 elements.

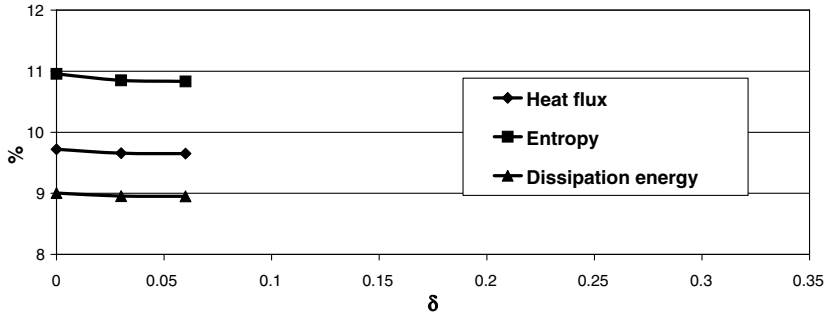

Fig. 12. The norm $\delta q_n, \delta\sigma_c, \delta\Psi_c$ as functions of the distance δ from the boundary $y = 0$ along internal line of intersection $x = 0.5$ for FEM with 144 elements.

The classic FEM leads to much worse results than the FEMT because the latter makes use of the Trefftz functions that satisfy the energy equation. This way the physical meaning of the results is ensured. Moreover, minimizing the numerical defect of energy dissipation or numerical entropy production on the borders between elements we do not "force" the solution to be continuous between elements. However, thanks to introducing the term that has a character of a penalty function and vanishes for continuous solution, the discontinuities are almost negligible and the physical character of the solution is preserved.

5. Inaccurate input data in the FEMT

To analyse an effect of the input data inaccuracy on the results in FEMT we introduce a disturbance (not exceeding 1% of the exact value) to the temperature obtained from the formula (20) and then used as an input data in the above presented analysis. Thus, the given temperature is obtained from the formula

$$T_{\text{inacc}}(x,y) = \frac{\cos\left(\frac{\pi}{2}x\right)\sinh\left(\frac{\pi}{2}(1-y)\right)}{\sinh\left(\frac{\pi}{2}\right)} \cdot \left(1 + \frac{\sigma(1-y)}{100}\right) \qquad (25)$$

with $|\sigma| \leqslant 1$ standing for a random error.

Table 9
Norm δH^1 as a function of the distance δ from the boundary $y = 0$ (12 base functions in an element) for inaccurate input data

δ	Pointwise continuous FEMT		
	$\alpha = 0.001$	$\alpha = 1$	$\alpha = 1000$
0.00	1.05	1.27	1.35
0.10	2.82	3.37	2.65
0.20	5.98	6.52	11.06
0.30	12.55	25.17	69.09
0.40	86.82	29.68	30.83
0.50	115.18	42.95	43.46
0.60	43.58	171.41	4.64
0.70	37.04	46.55	22.83
0.80	15.22	200.57	49.98
0.90	33.79	83.37	56.17
0.95	42.17	15.31	18.23
0.99	7.57	3.98	1.48

In order to illustrate an influence of such a disturbance for calculation stability let us notice that for fixed x the function $T_{\text{inacc}}(x, y)$ is an exponential function of the variable y. It means that along the y-axis an inaccuracy of the input data (temperature at some internal points) is enhanced exponentially. It is much worse situation than in the 1D case, because then an inaccuracy is enhanced linearly.

The pointwise continuous FEMT (12 base functions in the element) applied to inaccurate input data produced for $x = \delta$ according to formula (25) obviously leads to the inaccurate results. The norm δH^1 as a function of the distance δ from the boundary $y = 0$ is presented in Table 9.

The worst results are obtained on the border between elements. However, the results for $\delta \leqslant 0.3$ seem to be acceptable for the three analysed values of the parameter α. In the case of inaccurate input data the question of the most advantageous value of α seems to be more complex than in the case of the exact input data. However, the results presented in Table 9 suggest that for $\delta \leqslant 0.3$ small values of the parameter α are more advantageous for calculation than the greater ones.

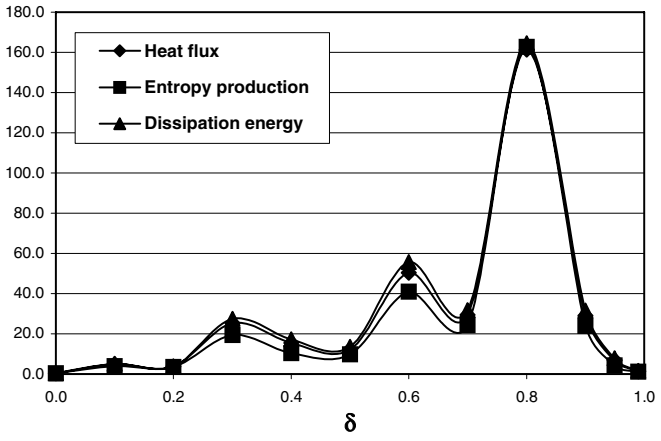

Fig. 13. The norm $\delta q_n, \delta\sigma_c, \delta\Psi_c$ as functions of the distance δ from the boundary $y = 0$ along internal line of intersection $x = 0.5$ for $\alpha = 1$ (FEMT pointwise continuous, 12 base functions in an element).

Errors of the heat flux, entropy production and energy dissipation on the border between elements for the intersection $x = 0.5$ as functions of parameter α and distance δ are presented in Fig. 13. The norms $\delta q_n, \delta\sigma_c, \delta\Psi_c$ do not exceed 3.8% for $\delta \leqslant 0.2$; for greater values of δ they rise to achieve their maximum for $\delta = 0.8$. Also in this case the stabilising role of the Trefftz functions is observable.

6. FEMT versus other methods of solving the inverse problems

FEM with Trefftz base functions applied to the test problems with accurate input data in 1D and 2D leads to almost exact results both, for direct as well as for inverse problem. The term that has a character of a penalty function and vanishes for continuous solution regularises the solutions and the parameter α is something like a regularising parameter. Moreover, to find a proper value of the parameter does not seem to be difficult. This is the most important difference between the FEMT and – for an instance – the Tikhonov regularisation method.

The Tikhonov method is sometimes combined with physical circumstances. One can find such combination in a paper of Dulikravitch et al. [6], in which a formulation for the inverse determination of unknown steady boundary conditions in heat conduction and thermoelasticity for three-dimensional problems was developed using FEM and three regularization methods (all of them based on Tikhonov regularisation). One of them uses Laplacian smoothing of the unknown temperatures and displacements only on the boundaries where the boundary conditions are unknown. This method could be considered a "second order" Tikhonov method.

The Generalized Eigensystem techniques was developed for solving inverse boundary value problem in steady heat conduction, and found out that the vector expansion methods often give superior results to those obtained with standard Tikhonov regularization method (comp. [7]). However, the method has rather mathematical than physical background.

Many mathematical methods that are employed to solve the inverse problem, e.g. a gradient-based inverse method combined with B-spline function specification (comp. [8]), the truncated singular value decomposition (SVD) method often used to solve this ill-conditioned system of algebraic equations (comp. [9]), and many others. However, practically almost none of them exploits physics in order to regularise an approximate solution.

The use of Trefftz functions as base functions in FEMT ensures physical meaning of the results and therefore seems to be more efficient that the use of polynomial base functions. This way, independently of inaccuracies of the input data, the approximate solution cannot be totally wrong, because it consists of the functions satisfying the energy equation.

7. Final remarks

In the analysed inverse problem, minimizing the numerical entropy production defect, energy dissipation or heat flux defect on the border between elements practically leads to the same results. Minimizing the heat flux jump between elements ensures less sensitivity of the approximate solution of an inverse problem on the thermoelement location. In other words we minimize the numerical energy defect caused by the finite number of base functions.

Notice that entropy production functional and energy dissipation functional are not quadratic functions of the coefficients at the base functions in elements. Hence, minimizing the functionals leads to non-linear system of algebraic equations. It seems to be the only disadvantage of the approach presented in this paper when compared with minimizing mean-square defects of heat flux (formula (18)); the latter leads to linear system of equations.

Acknowledgements

The presented paper is partially a result of the first author's cooperation with TU Dresden within the framework of the Humboldt Scholarship and was next developed within the KBN 3T 10B 060 27 Grant.

References

[1] A. Bejan, Entropy Generation through Heat and Fluid Flow, A Wiley-Interscience Publication John Wiley & Sons, 1994.
[2] M. Ciałkowski, A. Frąckowiak, Heat Functions and Their Application to Solving Heat Conduction and Mechanical Problems, Wydawnictwo Politechniki Poznańskiej, Poznań, 2000 (in Polish).
[3] M. Ciałkowski, The principle of minimum entropy production applied to solving inverse problems of heat conduction, in: XII Sympozjum Wymiany Ciepła i Masy, Kraków, 2004 (in Polish).
[4] B. Cockburn, Discontinuous Galerkin methods, ZAMM (2003) 731–754.
[5] O.C. Zienkiewicz, R.L. Taylor, S.J. Sherwin, J. Peiro, On discontinuous Galerkin methods, Int. J. Numer. Meth. Eng. 58 (2003) 1119–1148.
[6] B.H. Dennis, G.S. Dulikravich, Yoshimura Shinobu, A finite element formulation for the determination of unknown boundary conditions for 3-D steady thermoelastic problems, ASME J. Heat Transfer 126 (February) (2004), see also http://cfdlab.uta.edu/~brian/papers/JHT-INVERSE03.pdf.
[7] R. Throne, L. Olson, The steady inverse heat conduction problem: a comparison of methods with parameter selection, J. Heat Transfer 123 (August) (2001) 633–644.
[8] Sun Kyoung Kim, Woo II Lee, Inverse estimation of steady-state surface temperature on a three-dimensional body, Int. J. Numer. Meth. Heat Fluid Flow 12 (8) (2002) 1032–1050.
[9] T.J. Martin, G.S. Dulikravich, Inverse determination of steady heat convection coefficient distributions, Trans. ASME 120 (Mai) (1998) 328–334.